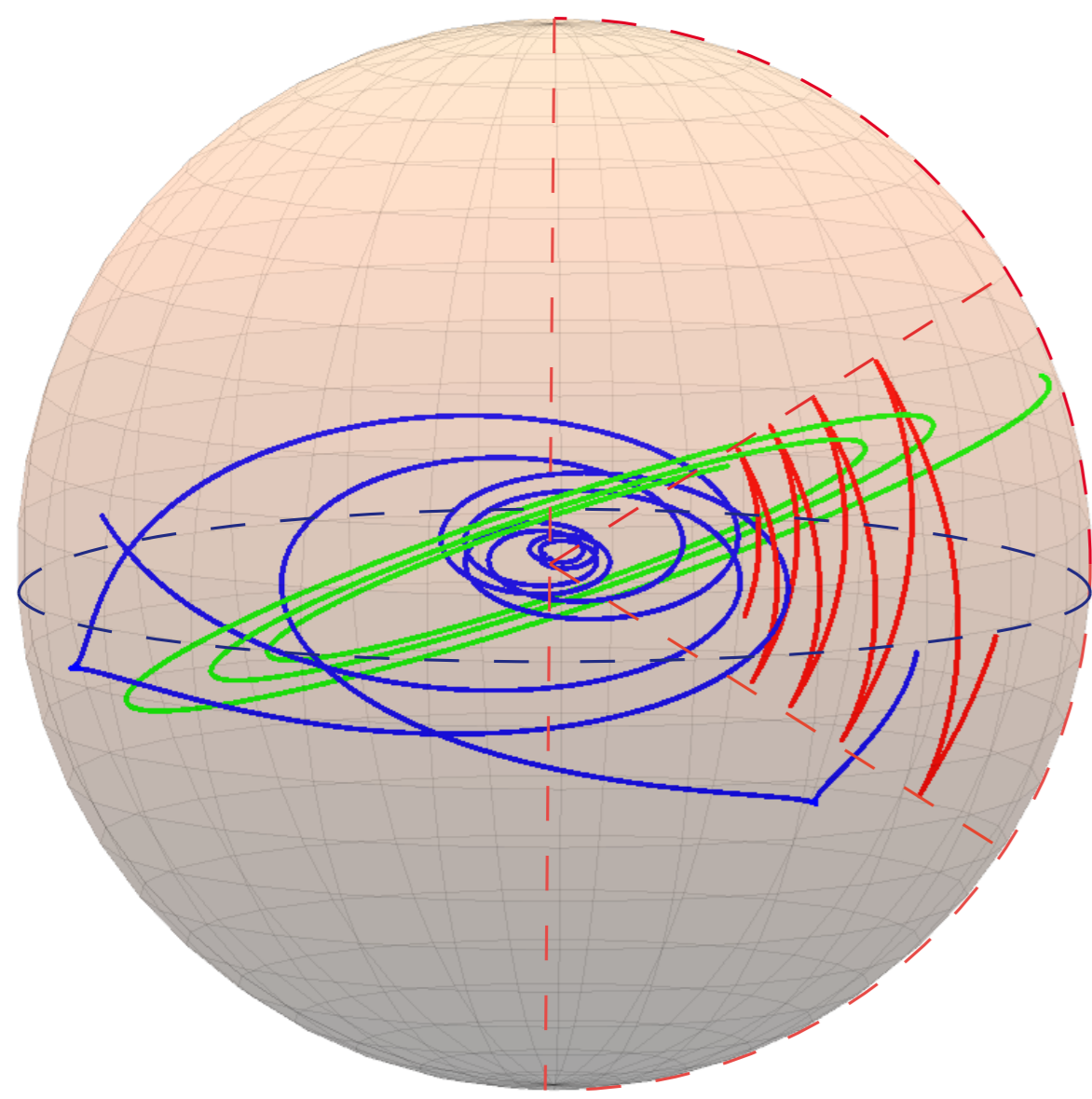


Abstract

We perform numerical simulations of a full solar-like star (from $r=0$ to $r=0.97R_{\odot}$) using the 3D anelastic ASH code. Due to the pummeling of convective plumes at the interface with the radiative zone, a rich spectrum of internal gravity waves is excited. We study its properties and find a good agreement with the linear and asymptotic theories, but also some differences due to nonlinear effects. In the physical space, low frequency waves are the most visible because of their high amplitude. By imposing a frequency filter to the signal in the radiative zone, we are able to visualize the path of gravity waves at different frequencies. Combining these observations with the results provided by our 3D raytracing code, we can identify the spatial localization of the resonant modes in the spherical radiative region. This method has several possible applications such as helping us to distinguish between propagative waves and standing modes or revealing the equatorial trapping of sub-inertial gravito-inertial waves in rotating stars.

Introduction

Gravity waves propagate and enter resonance in radiation zones of stars. Thanks to their dispersion relation : $\omega^2 = \frac{1}{k^2} \left[N^2 k_h^2 + (2\Omega \cdot k)^2 \right]$, where ω is the frequency of the wave, N the Brunt-Väisälä frequency measuring the density stratification of the fluid, k the wavevector (k_h its horizontal component) and Ω the rotation rate of the star, we can compute the raypaths of gravito-inertial waves in 2D (see e.g. Gough, 1993) but also in 3D (Fig. 1).



Depending on their frequencies and wavenumbers, individual gravity waves propagate in different planes and directions in the sphere. **The motivation of this work is to explore, in the physical space, the richness of a full gravity waves spectrum, excited by turbulent convection.**

Fig. 1 : 3D computation of gravity waves raypaths. Green ray : $\omega = 0.016$ mHz, $\ell=6$, $m=6$. Blue ray : $\omega = 0.1$ mHz, $\ell=5$, $m=4$. Red ray : $\omega = 0.003$ mHz in a star rotating at $10\Omega_{\odot}$ (sub-inertial wave).

3D nonlinear simulation of a solar-type star : Excitation of a rich spectrum of internal gravity waves

We here present results obtained with the anelastic spherical harmonic (ASH) code (Brun et al. 2004). Our model nonlinearly couples the convective envelope to the stable radiative core of the Sun (Brun et al. 2011), assuming a realistic solar stratification from $r = 0$ up to $0.97R_{\odot}$. The pummeling of convective plumes at the top of the radiative zone generates a rich spectrum of IGWs up to the maximum Brunt-Väisälä frequency (≈ 0.45 mHz) that includes both **standing and propagative waves** (see Alvan et al. 2014 for more details). This work generalizes the results by Rogers & Glatzmaier (2005) obtained in 2D.

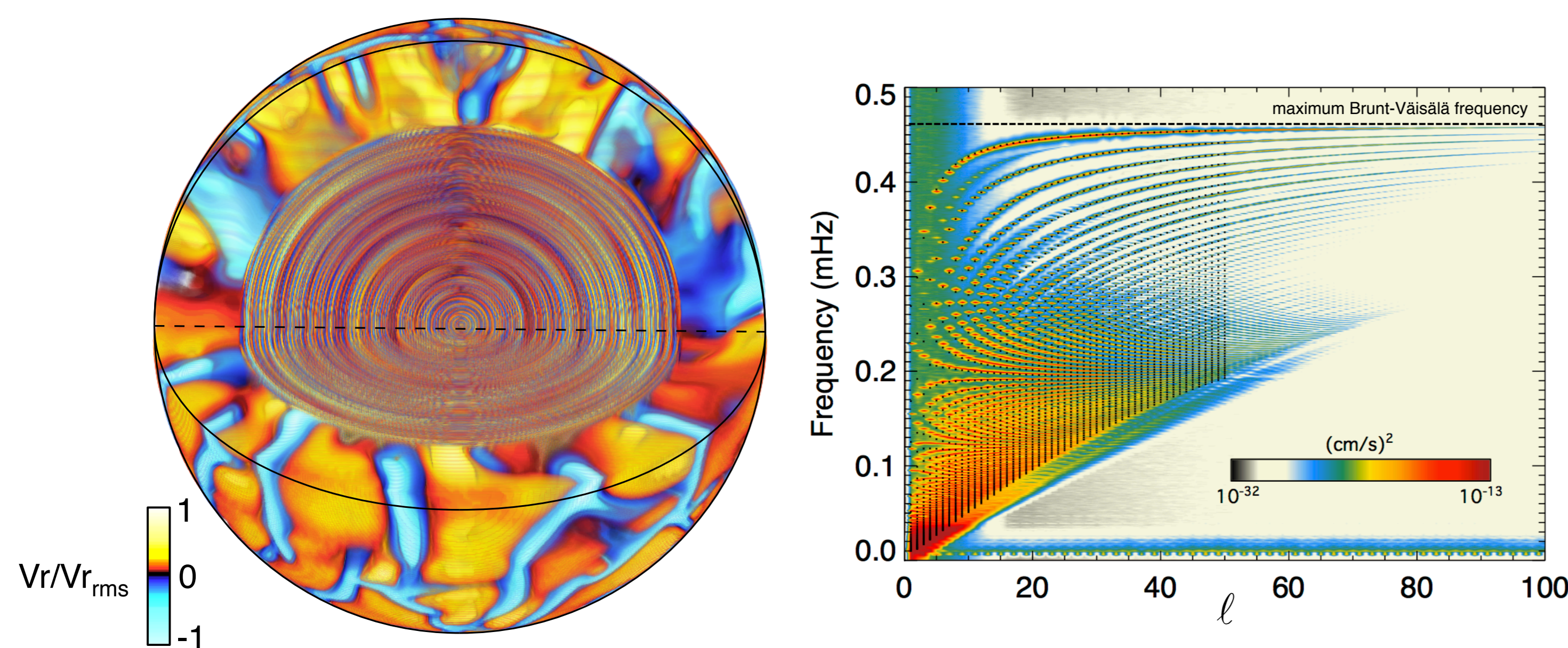


Fig. 2 : Left : 3D view of the simulated star. We see convective patterns (outer zone) and wavefronts (inner radiative zone). **Waves spiral towards the center with a pattern characteristic of low-frequency gravity waves.** Right : Spectrum of gravity waves calculated at $r = 0.26R_{\odot}$ (middle of the radiative zone). We represent the radial kinetic energy $E(r_0, \ell, \omega)$ as a function of the order ℓ and frequency ω . Black crosses mark the pulsations frequencies predicted by the ADIPLS oscillation code (Christensen-Dalsgaard, 2011). **This spectrum shows that a broad range of frequencies are excited, that are not directly visible in the physical space (left panel).**

Frequency filtering

The wave pattern visible in the left panel of Fig. 1 is not representative of the richness of the spectrum. In order to visualize individual waves, we apply a pass-band filter in the Fourier space to select a narrow band of frequencies.

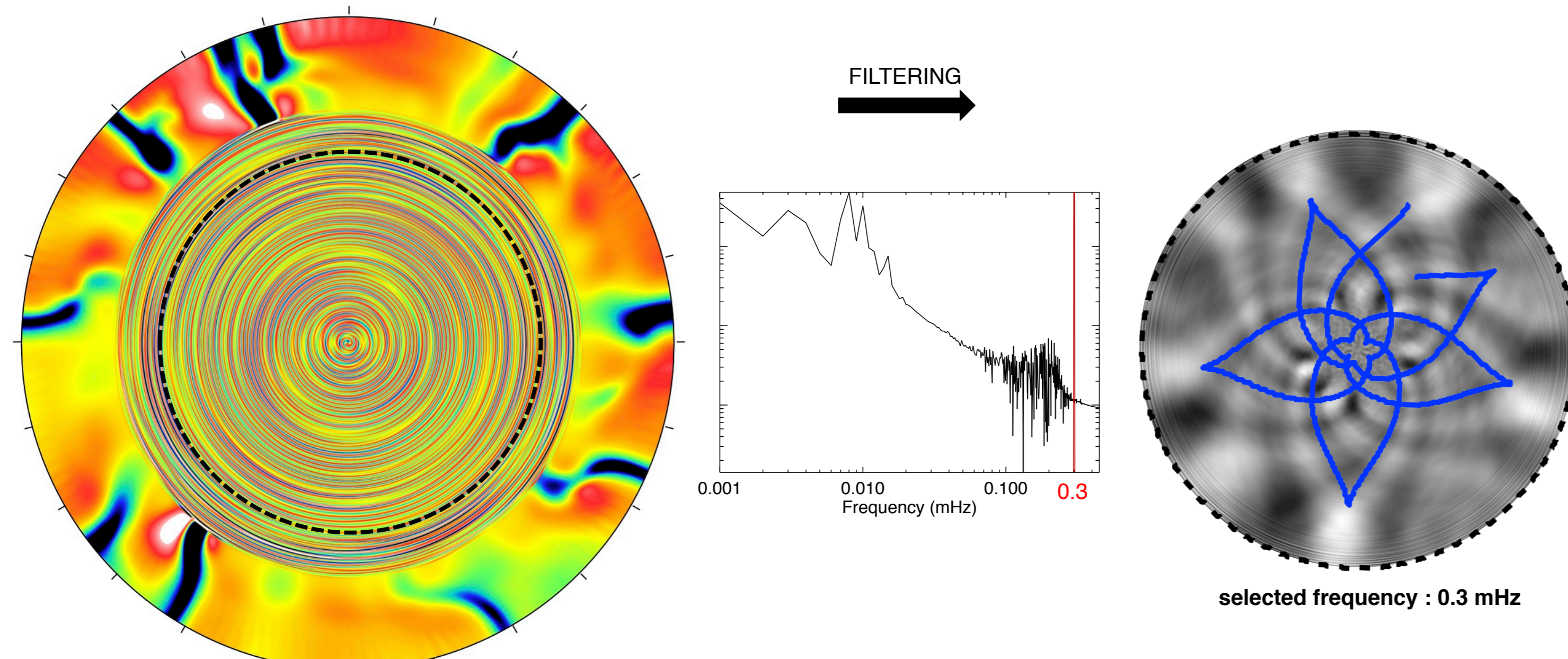


Fig. 3 : Left : Equatorial slice of the 3D model ($V_r/V_{r,rms}$) presented in Fig. 2. Middle : Exemple of a Fourier spectrum of one point of the radiative zone, calculated with a time serie of about 11 days. The most powerful part corresponds to low frequencies. We filter the signal and retain frequencies around 0.3 mHz (red curve). Right : Equatorial view after filtering. The pattern observed corresponds to the one predicted by the raytracing theory (blue line).

Application 1 : Propagative waves and standing modes

One possible application of this filtering method is to **distinguish between propagative waves (damped along their propagation) and standing modes (which resonate in the sphere)**. In the figure below, where we have filtered the same signal at two different frequencies, we see that waves propagate along beams forming an angle with respect to the vertical (St Andrew's crosses). The more the frequency increases, the more the beams are vertically oriented. **Low-frequency propagative waves in the right panel disappear after $0.55R_{\odot}$, damped by thermal effects (Zahn et al. 1997).**

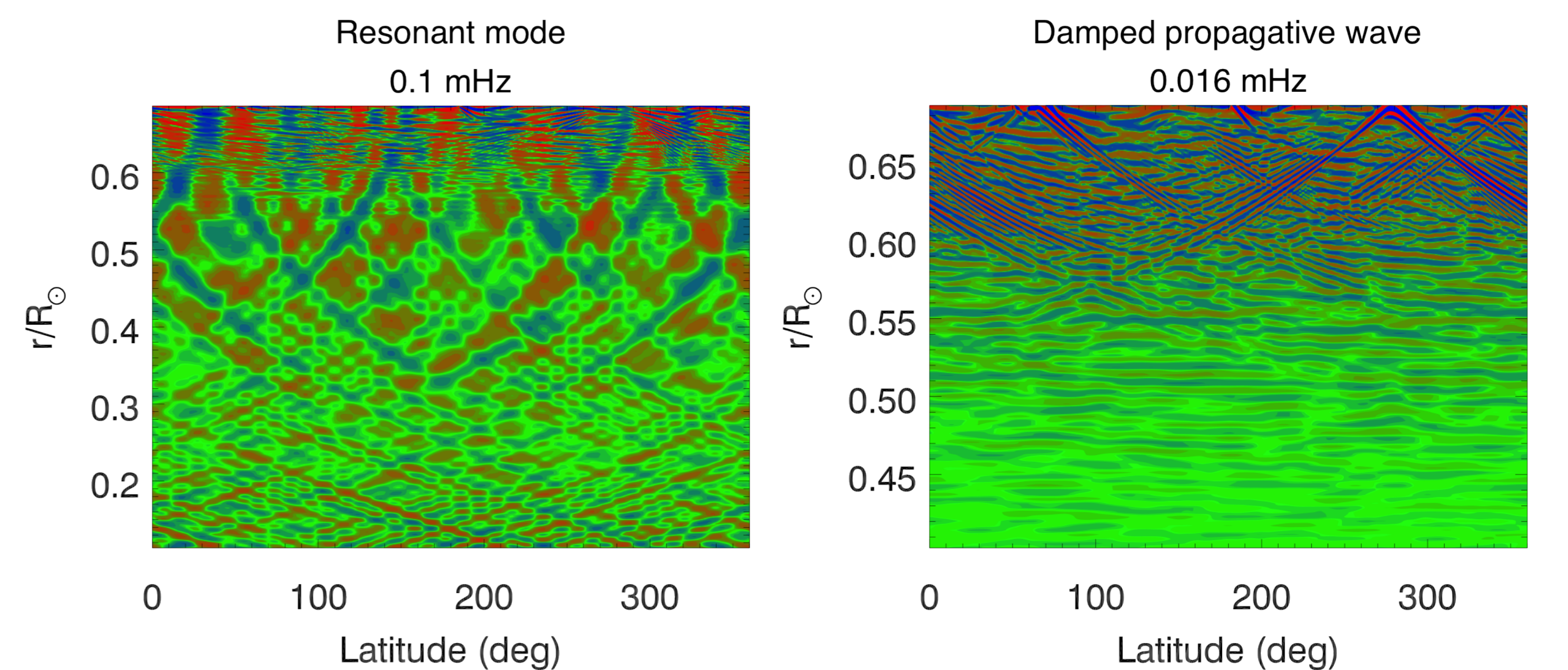


Fig. 4 : Left : Equatorial plane filtered at $\omega = 0.1$ mHz. Rays propagate towards the center with a weak attenuation and form standing modes (blue ray in Fig. 1). Right : Same plane filtered at $\omega = 0.016$ mHz. The wave beams are rapidly damped so they can not reach the center and form modes. The raypath corresponds to the green one in Fig. 1, except that the adiabatic raytracing theory can not show the thermal damping affecting the wave's amplitude.

Application 2 : Equatorial trapping due to rotation

Here, we use a simplified model where the convection zone is not taken into account. Instead, we **excite gravity waves with a gaussian perturbation in entropy** centered in S (see Fig. 5). This reduced model allows us to reach a broader range of parameters. The model presented here is **rotating at $\Omega = 100\Omega_{\odot} = 0.4\Omega_K$** , where Ω_K is the break-up rotation rate. By filtering the **polar plane** at $\omega_{super} > 2\Omega$ and $\omega_{sub} < 2\Omega$, we observe super-inertial waves (left) and sub-inertial waves (right) which are **equatorially trapped**, due to the Coriolis acceleration. We do not take into account the centrifugal distortion, whose effects are discussed in Ballot et al. (2010).

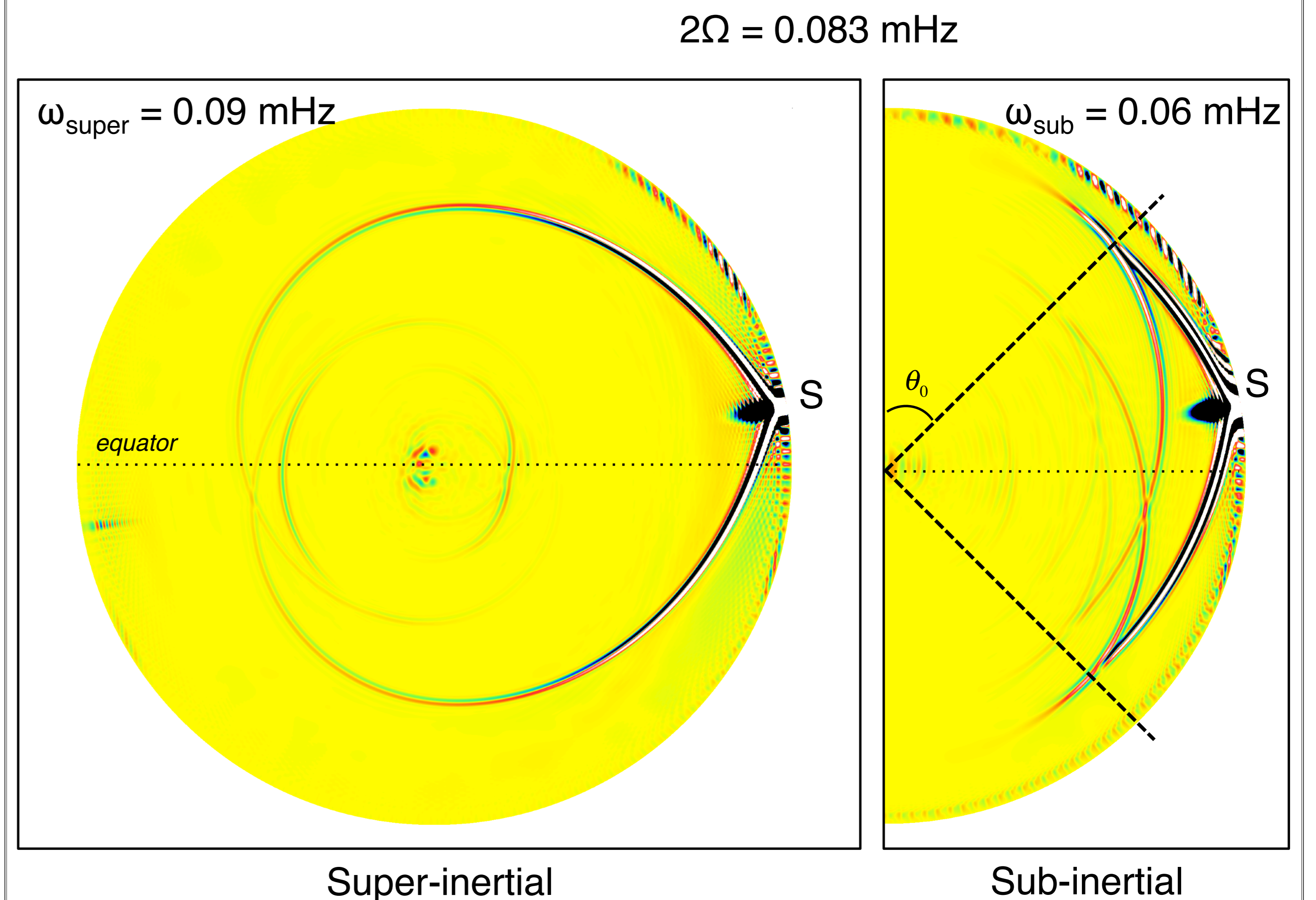


Fig. 5 : Left : Polar view of a super-inertial wave propagating from the source S. Right : Sub-inertial wave trapped in latitude. The relation predicted by the linear theory is respected : $\cos \theta_0 = \omega/2\Omega$, although we observe some energy transmission beyond the critical latitude. On both panels, we also see the thermal damping affecting the beam whose energy decreases along the propagation.

Conclusion

We propose a detailed analysis of IGWs in our 3D nonlinear dynamical simulations in Alvan et al. 2014, but this filtering method allows to go further and opens a large new range of possibilities. We can visualize individual waves and see the distinction between :

- standing modes and propagative waves, due to thermal effects
- super- and sub-inertial waves, as function of the rotation rate of the star

We are currently developing new models taking into account a velocity gradient deep in the radiative zone (instead of a flat profile) and we will be able to study both the effect of this differential rotation on waves and the angular momentum transport induced by IGWs (Mathis et al. 2014).